

Supplementary Information

Reactivity-Matched Synthesis of Monodisperse Ag(In,Ga)S₂ QDs with Efficient Luminescence

Naiwei Wei^{1,2}, Hong Zhu^{1,2}, Danni Yan^{1,2}, Shuai Yang^{1,2}, Lili Xu^{1,2}, Shengli Zhang¹,
², and Yuhui Dong^{1,2,*}, Yousheng Zou^{1,2,*}, Haibo Zeng^{1,2,*}

¹*Institute of Optoelectronics & Nanomaterials, College of Materials Science and Engineering, Nanjing University of Science and Technology, Nanjing 210094, China*

²*Key Laboratory of Advanced Display Materials and Devices, Ministry of Industry and Information Technology, Nanjing 210094, China*

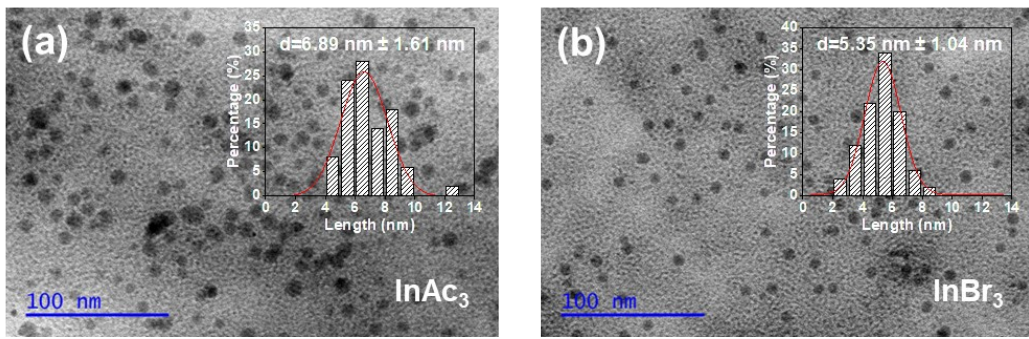


Fig. S1 TEM images and the corresponding size distribution histograms of the AIGS QDs synthesized using InAc_3 and InBr_3 , respectively.

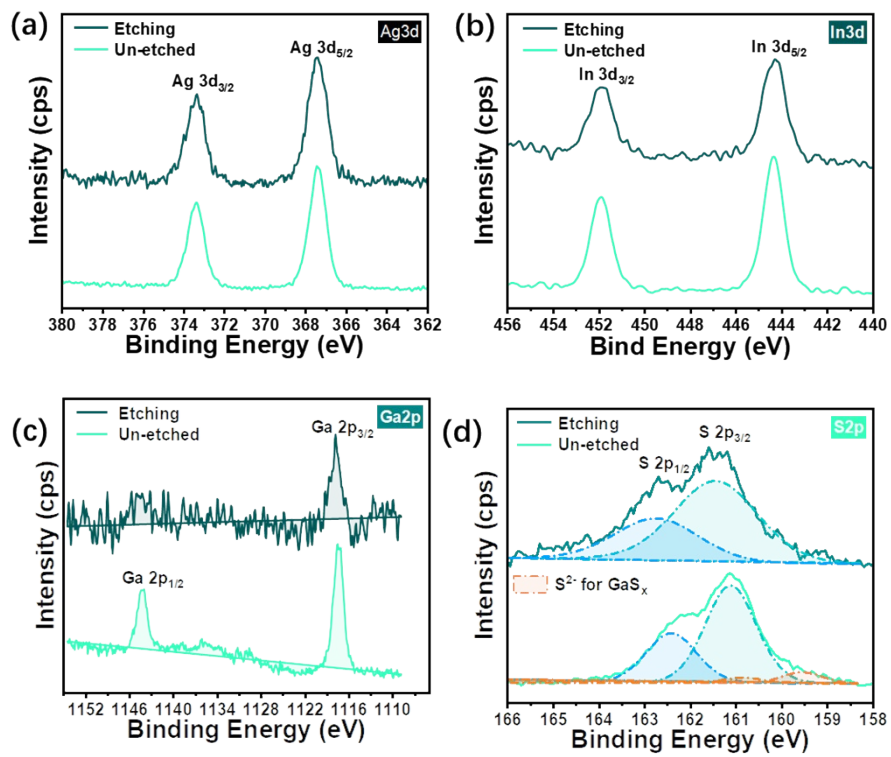


Fig. S2 XPS spectra of AIGS@ GaS_x core/shell QDs for (a) Ag 3d, (b) In 3d, (c) Ga 2p, and (d) S 2p regions synthesized using InI_3 before and after etching.

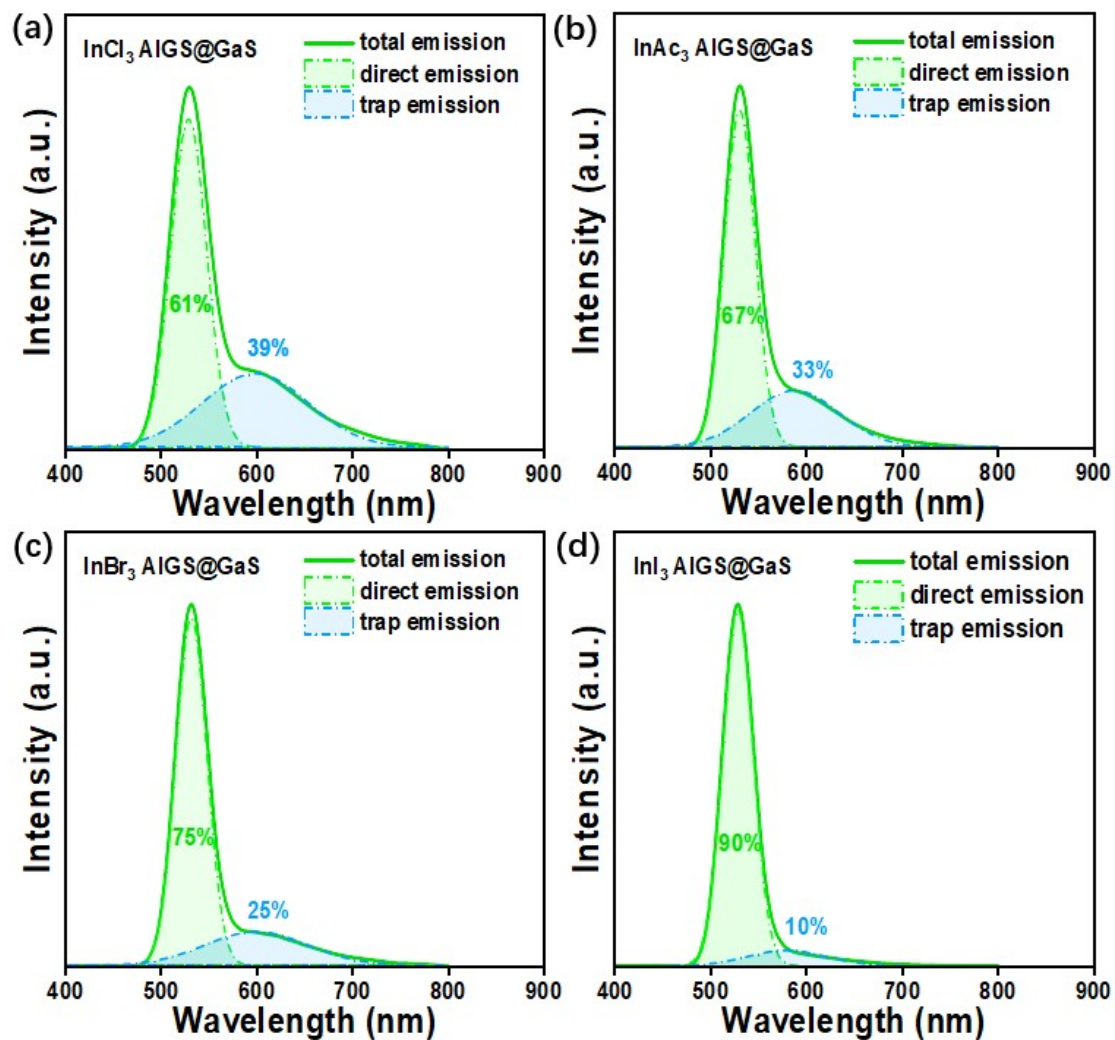


Fig. S3 Fitted PL spectra of the AIGS QDs synthesized using (a) InCl_3 , (b) InAc_3 , (c) InBr_3 , and InI_3 , respectively.

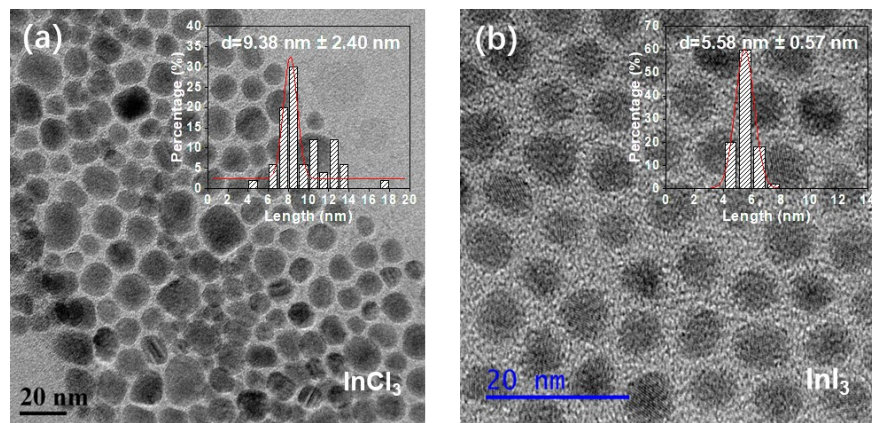


Fig. S4 TEM images of the AIGS@GaS_x QDs synthesized using InCl_3 and InI_3 , respectively.

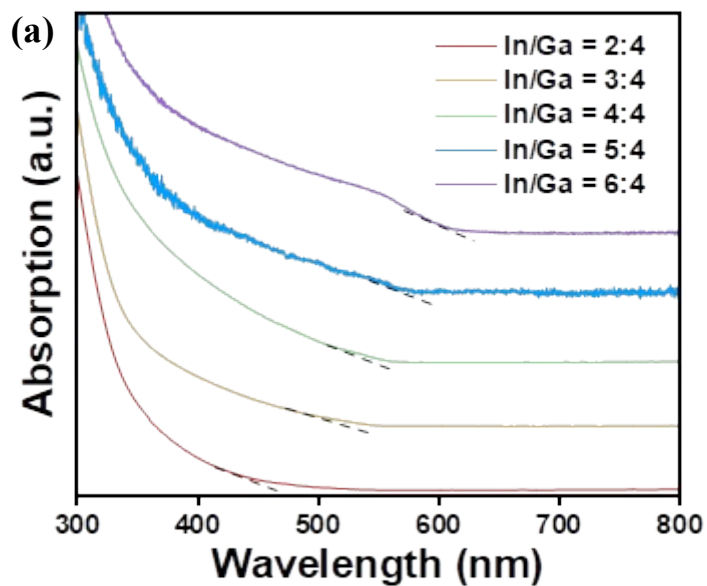


Fig. S5 Absorption curves of AIGS@GaS_x core/shell QDs with different In/Ga ratios.

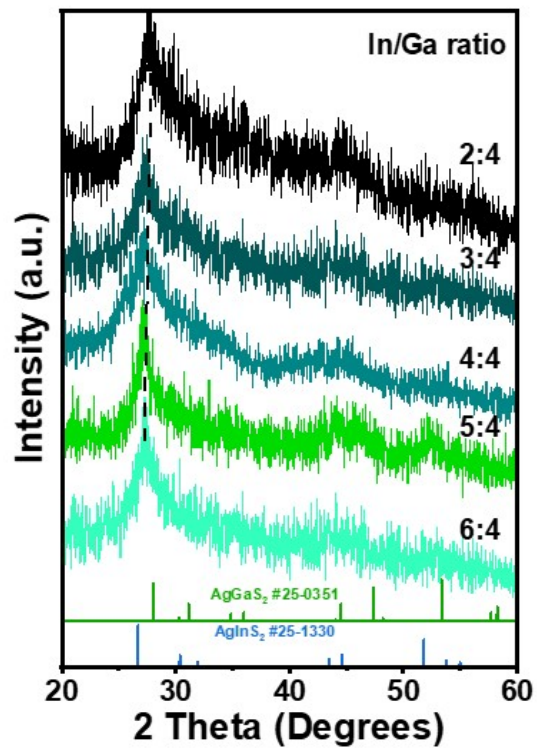


Fig. S6 XRD spectra of the AIGS/GaS_x core/shell QDs with In/Ga molar ratios of 2:4, 3:4, 4:4, 5:4, and 6:4 synthesized with the same metal salt InI₃.

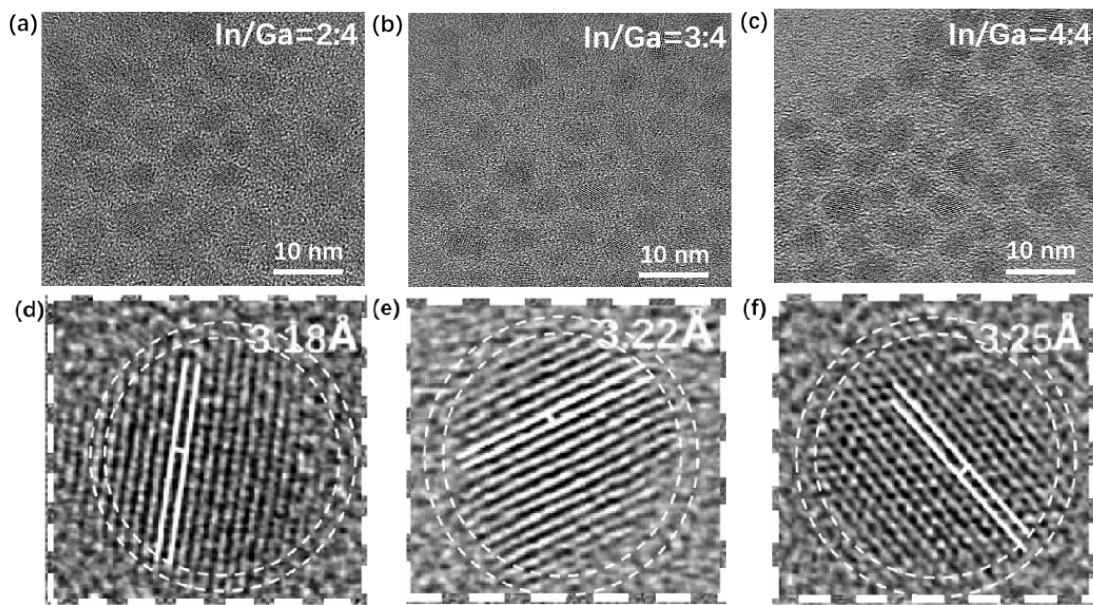


Fig. S7 TEM image of the AIGS/GaS_x core/shell QDs with In/Ga molar ratios of (a) 2:4, (b) 3:4, (c) 4:4, HRTEM image of the AIGS/GaS_x core/shell QDs with In/Ga molar ratios of (d) 2:4, (e) 3:4, and (f) 4:4.

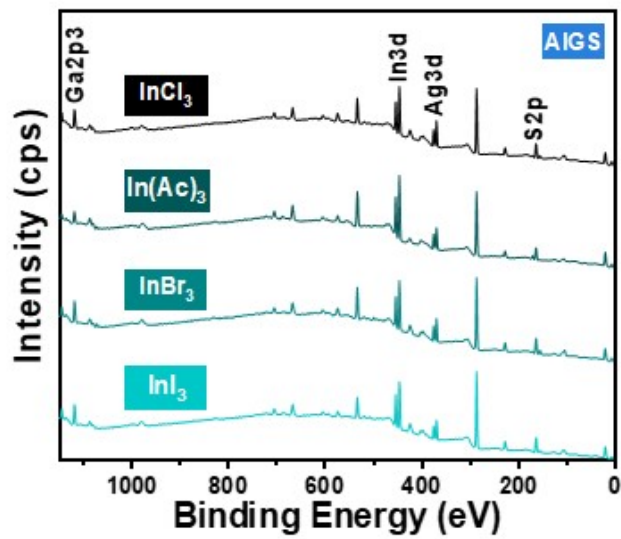


Fig. S8 XPS spectra of AIGS QDs synthesized using InCl_3 , $\text{In}(\text{Ac})_3$, InBr_3 , and InI_3 , respectively.

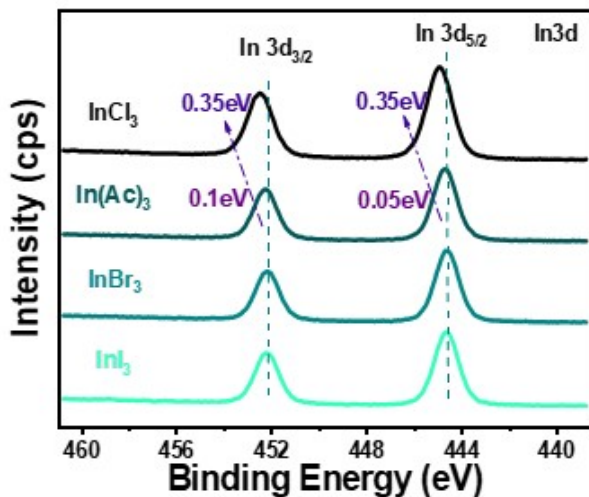


Fig. S9 XPS spectra of AIGS QDs for In 3d regions synthesized using difference In sources.

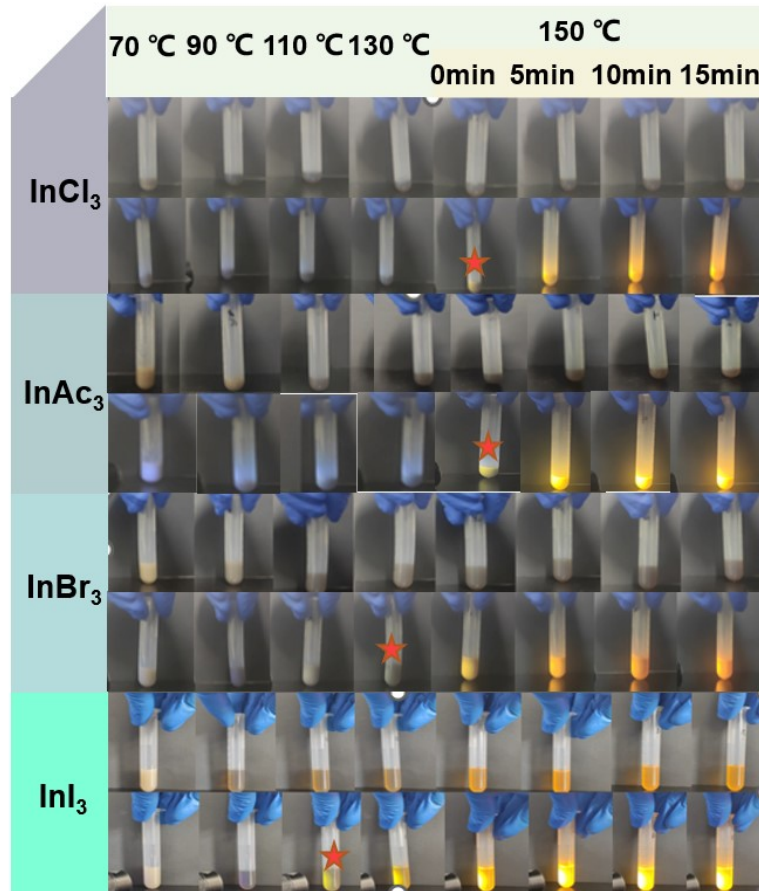


Fig. S10 Photographs for reaction stage under white light (upper photos) and UV light (bottom photos) extracts from 70 °C to 150 °C 15 min of AIGS QDs synthesized using InCl_3 , InAc_3 , InBr_3 , and InI_3 , respectively.

Table S1. Elements Hard and Soft Acid and Base (HSAB) diagram.

Acid	Base	Hard base	Junction base	Soft base
		$\text{CH}_3\text{COO}^- \cdot \text{Cl}^-$	Br^-	I^-
Hard acid	In^{3+}	Strong bond	Relatively strong bond	Weak bond

Table S2. Calculated bond formation energies from In(A)_3 to In^{3+} ($\text{A} = \text{Cl}^-$, Ac^- ,

Br^- , I^-)

	InCl_3	InAc_3	InBr_3	InI_3
E_{form}	1.01 eV	2.59 eV	0.86 eV	0.50 eV

Table S3. Average lifetimes and radiative composite and nonradiative occupancies of AIGS QDs synthesized using InCl_3 , InAc_3 , InBr_3 , and InI_3 , respectively.

AIGS	$\langle \tau_{\text{av}} \rangle$ (ns)	τ_1 (ns)	τ_2 (ns)	f_1	f_2
InCl_3	177.92	28.04	214.55	73.19%	26.81%
InAc_3	175.41	34.79	203.90	57.69%	42.31%
InBr_3	181.94	38.52	208.46	45.21%	54.79%
InI_3	197.24	42.70	223.08	38.22%	61.78%

Table S4. Element atom % of QD and etch-QD analyzed by XPS.

Sample	Element atom %				
	Ag	In	Ga	Ag+In+Ga	S
QD	11.88	5.49	17.43	34.80	65.20
Etch-QD	18.18	9.09	5.84	33.11	66.89

Table S5. Average lifetimes and radiative composite and nonradiative occupancies

of AIGS@GaS_x QDs synthesized using InCl₃, InAc₃, InBr₃, and InI₃, respectively.

AIGS@GaS _x	$\langle \tau_{av} \rangle$ (ns)	τ_1 (ns)	τ_2 (ns)	τ_3 (ns)	f_1	f_2	f_3
InCl ₃	106.03	6.89	41.83	207.60	5.01%	33.37%	61.62%
InAc ₃	99.01	7.85	44.54	189.75	8.09%	37.66%	54.25%
InBr ₃	84.63	5.92	35.51	133.64	7.45%	46.38%	46.17%
InI ₃	76.66	4.35	26.86	157.10	8.55%	54.69%	36.76%

Table S6. Summary of properties based on I-III-VI and derivative QDs.

QDs	PL (nm)	FWHM (nm)	Colour	PLQY (%)	Ref
AIS@GaS _x	600	30	Yellow	56%	1
AIS@GaS _x	~580	~33	Yellow	72.3	2
AIS@GaS _x	560	45	Yellow	26.7	3
AIS@GaS _x	530	~37	Green	40	4
AIS@GaS@ZnS	575	~48	Yellow	~60	5
AIGS@GaS _x	530	41	Pure-Green	~28	6
AIGS@GaS _x	568	36	Yellow	71	7
AIGS@GaS _x	518	36	Green	68	8
AIGS@GaS _x	543	37	Green	99	9
AIGS@GaS _x	528	31	Pure-Green	53	9
AIGS@AGS	517	30	Green	96	10
AIGS@GaS_x	530	31	Pure-Green	90	This work

References

- 1 T. Uematsu, K. Wajima, D. K. Sharma, S. Hirata, T. Yamamoto, T. Kameyama, M. Vacha, T. Torimoto, S. Kuwabata, *NPG Asia Mater.* 2018, **10**, 713.
- 2 W. Hoisang, T. Uematsu, T. Yamamoto, T. Torimoto, S. Kuwabata, *Nanomaterials*. 2019, **9**, 1763.
- 3 G. Motomura, K. Ogura, Y. Iwasaki, T. Uematsu, S. Kuwabata, T. Kameyama, T. Torimoto, T. Tsuzuki, *Appl. Phys. Lett.* 2020, **117**, 091101.
- 4 T. T. T. Huong, N. T. Loan, T. D. T. Ung, N. T. Tung, H. Han, N. Q. Liem, *Nanotech.* 2022, **33**, 355704.
- 5 N. T. Loan, T. T. T. Huong, M. A. Luong, L. Van Long, H. Han, T. D. T. Ung, N. Q. Liem, *Nanotech.* 2023, **34**, 315601.
- 6 T. Kameyama, M. Kishi, C. Miyamae, D. K. Sharma, S. Hirata, T. Yamamoto, T. Uematsu, M. Vacha, S. Kuwabata, T. Torimoto, *ACS Appl. Mater. Interfaces*. 2018, **10**, 42844.
- 7 W. Hoisang, T. Uematsu, T. Torimoto, S. Kuwabata, *Chem. Lett.* 2021, **50**, 1863.
- 8 W. Hoisang, T. Uematsu, T. Torimoto, S. Kuwabata, *Inorg. Chem.* 2021, **60**, 13101.
- 9 T. Uematsu, M. Tepakidareekul, T. Hirano, T. Torimoto, S. Kuwabata, *Chem. Mater.* 2023, **35**, 1094.
- 10 H. J. Lee, S. Im, D. Jung, K. Kim, J. A. Chae, J. Lim, J. W. Park, D. Shin, K. Char, B. G. Jeong, J.-S. Park, E. Hwang, D. C. Lee, Y.-S. Park, H.-J. Song, J. H. Chang, W. K. Bae, *Nat. Commun.* 2023, **14**, 3779.